Available online at www.sciencedirect.com
ScienceDirect
Polymer 48 (2007) 7356–7363
polymer
www.elsevier.com/locate/polymer

Effect of aging time on the volumetric and enthalpic glass transition of *a*-PMMA upon heating

P. Riha [a,*], J. Hadac [b], P. Slobodian [b], P. Sáha [b], R.W. Rychwalski [c], J. Kubát [b,c]

[a] *Institute of Hydrodynamics, Academy of Sciences of the Czech Republic, 16612 Prague, Czech Republic*
[b] *Tomas Bata University, Faculty of Technology, Polymer Centre, 76272 Zlin, Czech Republic*
[c] *Chalmers University of Technology, Materials and Manufacturing Technology, 412 96 Gothenburg, Sweden*

Received 19 March 2007; received in revised form 29 August 2007; accepted 4 September 2007
Available online 8 September 2007

Abstract

In this paper we model the volumetric and enthalpic response of *a*-PMMA during heating at constant rate through the glass transition region following an aging period of varying length. The modeling is based on a recently developed thermodynamically consistent non-linear viscoelastic theory of thermal and mechanical behaviors of glassy polymers in the glass transition range [Caruthers JM, Adolf DB, Chambers RS, Shrikhande P. Polymer 2004;45:4577–97. Adolf DB, Chambers RS, Caruthers JM. Polymer 2004;45:4599–621]. The original model is slightly modified by replacing the stretched exponential by a relaxation function based on a simplified cooperative model emulating the commonly observed linear variation of the relaxing quantity with logarithmic time. Good agreement is found with the observed temperature dependence of specific volume and enthalpy. Also the peaks in thermal expansivity and heat capacity are well described, both with regard to their intensity and position along the temperature axis.

Keywords: *a*-PMMA; Glass transition; Aging

1. Introduction

In contrast to the equilibrium of a rubbery polymer, the non-equilibrium glassy state is associated with time-dependent processes known as physical aging. Basically, aging is the approach to equilibrium of a disturbed system accompanied by changes in thermodynamic, mechanical and other physical properties. Measurements of the temperature and time dependence of the specific volume, $v = 1/\rho$, and specific enthalpy, h, around and below the glass temperature, T_g, belong to commonly used tools employed in studying aging phenomena. To emulate the $h(T)$ and $v(T)$ behavior after varying periods of aging, several semi-empirical concepts have been proposed. Among these the models known under their acronyms as TNM (Tool–Narayanaswamy–Moynihan), AGV (Adam–Gibbs–Vogel), and KAHR (Kovacs–Aklonis–Hutchinson–Ramos) appear to have reached a high level of acceptance in reproducing experimental facts. It may suffice here to refer to a recent paper by Simon and Bernazzani [1] commenting on the TNM and KAHR models. Relatively recent is also an article by Andreozzi et al. [2] applying the TNM and AGV approaches to DSC thermograms.

As discussed in Ref. [1] the structure of the models mentioned above includes several empirical features, especially with regard to thermodynamic aspects. A few years ago a thermodynamically consistent non-linear viscoelastic formalism has been proposed to describe the behavior of amorphous polymers in terms of thermophysical parameters and their temperature dependence [3,4]. According to this theory, based on rational mechanics, the non-linearities associated with the transition between rubbery and glassy states are not the result

* Corresponding author. Tel.: +420233109093; fax: +420233324361.
E-mail addresses: riha@ih.cas.cz (P. Riha), slobodian@ft.utb.cz (P. Slobodian).

0032-3861/$ - see front matter © 2007 Elsevier Ltd. All rights reserved.
doi:10.1016/j.polymer.2007.09.007

of using non-linear parameters, but rather a consequence of the thermodynamic constitutive framework. The theory employs a material clock based on the potential energy. The relaxation functions are represented by stretched exponentials.

In the present paper we employ the thermodynamic formalism according to Refs. [3,4] in order to emulate the $h(T)$ and $v(T)$ behavior of a-PMMA as observed during temperature upscans after different periods of aging. Apart from the $h(T)$ and $v(T)$ graphs also the corresponding peaks in the volumetric coefficient of thermal expansion, α_p, and the specific heat capacity, c_p, are included in the analysis.

The reader will note that we do not use the thermodynamic framework in its original form. The modification consists in replacing the stretched exponential used in Refs. [3,4] by a relaxation function resulting from a cooperative model [5–8] based on an induction mechanism formally analogous to that encountered in Bose–Einstein statistics. In a simplified form this amounts to replacing a simple time exponential $\exp(-\lambda t)$ with $1/[(1+\varepsilon)\exp(\lambda t)-1]$ in order to account for the non-exponentiality of the time derivative of the relaxing quantity. Omitting details given below one finds for $\varepsilon \ll 1$ and $t \ll 1/\lambda$ that this model is a way to reproduce the commonly observed linear dependence of the relaxing quantity on logarithmic time.

2. Thermodynamic formalism

The set of thermodynamic constitutive equations [3,4] recently proposed to capture the wide range of behaviors observed in amorphous polymers in connection with the glass transition are determined from the Helmholtz free energy using the rational mechanics framework and a material time scale. The Helmholtz free energy is approximated by a Frechet expansion in the temperature and strain histories about the equilibrated state at the current temperature and strain. The material clock is controlled by the potential energy contribution to the internal energy that is likewise determined from the Helmholtz free energy.

The original constitutive equations are reproduced below in the form used here to describe the glass transition in PMMA at atmospheric pressure. Owing to this condition the simplified equation for the stress can be written as:

$$0 = \boldsymbol{S}_{H_\infty} + \rho_{\mathrm{ref}}\psi_1 \int_0^t ds f_1(t^*-s^*)\frac{\mathrm{d}I_H}{\mathrm{d}s}(s)\boldsymbol{I} + \rho_{\mathrm{ref}}\psi_3(T,I_H)\int_0^t ds f_3(t^*-s^*)\frac{\mathrm{d}T}{\mathrm{d}s}(s)\boldsymbol{I}, \tag{1}$$

where the equilibrium contribution to stress:

$$\boldsymbol{S}_{H_\infty} = \boldsymbol{S}^{\mathrm{ref}}_{H_\infty} + \rho_{\mathrm{ref}}\psi_{II}I_H\boldsymbol{I} + \rho_{\mathrm{ref}}\psi_{IT}\Delta T\boldsymbol{I} + \frac{\rho_{\mathrm{ref}}}{2}\psi_{ITT}\Delta T^2\boldsymbol{I} + \rho_{\mathrm{ref}}\psi_{IIT}I_H\Delta T\boldsymbol{I}, \tag{2}$$

is balanced with the volume change (second term) and thermal stress (third term) in Eq. (1). The double integral terms appearing in the original constitutive scheme are neglected, since they have only a minimal effect on the stress constitutive equation [3]. In the above equations $\boldsymbol{S}^{\mathrm{ref}}_{H_\infty}$ denotes the equilibrated stress tensor in the reference state (atmospheric pressure), $\boldsymbol{I}$ the unit tensor, $I_H \approx (v-v_0)/v_0$ the first invariant of the Hencky strain, $\Delta T = T - T_{\mathrm{ref}}$ the temperature change, and the subscript or superscript ref the value at the reference temperature. The four Taylor series coefficients of the equilibrium contribution to stress $\psi_{II}, \psi_{IT}, \psi_{ITT}, \psi_{IIT}$ are defined in Ref. [4]. The coefficients are related to the thermophysical parameters of the material determined by independent experiments. Finally, ψ_1, ψ_3 denotes the prefactors and $f_k(t^*-s^*)(k=1,3)$ the normalized relaxation functions which depend upon backward looking material time (t^*-s^*).

The simplified equation for the specific entropy used to calculate the heat capacity is:

$$\eta = \eta_\infty - \psi_3(T,I_H)\int_0^t ds f_3(t^*-s^*)\frac{\mathrm{d}I_H}{\mathrm{d}s}(s) - \psi_4(T)\int_0^t ds f_4(t^*-s^*)\frac{\mathrm{d}T}{\mathrm{d}s}(s), \tag{3}$$

where the equilibrium contribution to the entropy, η_∞, is given by:

$$\eta_\infty = \eta^{\mathrm{ref}}_\infty - \psi_{IT}I_H - \frac{1}{2}\psi_{IIT}I_H^2 - \psi_{ITT}\Delta T I_H - \psi_{TT}\Delta T - \frac{1}{2}\psi_{TTT}\Delta T^2 - \frac{1}{6}\psi_{TTTT}\Delta T^3. \tag{4}$$

Again the double integral terms appearing in the original constitutive scheme are neglected, owing to a minimal effect on the Helmholtz free energy for isobaric processes and thus on the entropy [3]. The Taylor series coefficients of the equilibrium contribution to the entropy $\psi_{TT}, \psi_{TTT}, \psi_{TTTT}$ are introduced in Ref. [4] where their relation to the physical parameters determined by independent experiments is shown. Finally, ψ_4 denotes the prefactor and $f_4(t^*-s^*)$ the normalized relaxation function.

The prefactors ψ_k $(k=1,4)$ used for the solution of Eqs. (1) and (3) are the same as in Ref. [4]. However, $\psi_3(T,I_H)$ is expanded to higher order terms about the reference temperature and the reference volume than the corresponding one in Ref. [4], namely,

$$\psi_3(T,I_H) = \psi^{\mathrm{ref}}_3 + \left(\frac{\partial\psi_3}{\partial T}\right)^{\mathrm{ref}}_{I_H}\Delta T + \left(\frac{\partial\psi_3}{\partial I_H}\right)^{\mathrm{ref}}_{T} I_H + \frac{1}{2}\left(\frac{\partial^2\psi_3}{\partial T^2}\right)^{\mathrm{ref}}_{I_H}\Delta T^2 + \frac{1}{2}\left(\frac{\partial^2\psi_3}{\partial I_H^2}\right)^{\mathrm{ref}}_{T} I_H^2, \tag{5}$$

though the mixed derivative is not taken into account. The inclusion of the higher order expansion terms improves our data representation below the glass transition temperature in comparison with the use of the original $\psi_3(T,I_H)$ form given in Ref. [4].

3. The relaxation function based on a simplified cooperative model

Relaxation processes in solids or semi-solids are known to extend over a considerably broader range of logarithmic time than a process obeying first-order kinetics. This non-exponentiality, assumed to be related to cooperative effects, is often described using a stretched exponential function (KWW). Despite its frequent use, the physical background of this function has not been clarified. In the first place, this applies to the relation between the stretching exponent and the width of the corresponding spectrum of relaxation times.

Before the KWW function reached its current popularity, the so-called logarithmic time law stood out as a useful tool when describing the kinetics of stress or volume relaxation, primary creep, and other relaxation and recovery processes. The processes treated in this paper, that is volume and enthalpy relaxation, do not contradict the observation that the relaxing quantity varies linearly with logarithmic time over a significant range. Refs. [5–8] describe a highly simplified cooperative model which closely emulates this type of behavior. In this paper we use this model instead of the KWW function employed in Refs. [3,4]. This replacement is rather of a formal nature, since both descriptions necessarily must lead to similar results. However, it is our belief that the model to be used here provides a better transparency of the parameters determining the time evolvement of the quantities under investigation. The following brief outline of the basic features of the cooperative model may clarify such a view.

The model to be used is based on the idea that the elementary events contributing to the macroscopic process may occur in clusters of varying sizes due to an induction effect formally similar to that encountered in Bose–Einstein (B–E) statistics. Following Refs. [5–8] we thus start from the differential equation:

$$\frac{\mathrm{d}\dot{n}}{\mathrm{d}t} = \ddot{n} = -\lambda\dot{n}\left(1 - \frac{b}{\lambda}\dot{n}\right), \tag{6}$$

where λ denotes a rate constant ($= 1/\tau$), τ a relaxation time and b a parameter related to the extension of the process along the log t axis, that is to say to the degree of cooperativity. The symbol n is used in a general sense, denoting the macroscopic relaxing or recovering quantity. The term within the parenthesis in Eq. (6) represents the usual enhancement factor appearing in the same way in a B–E energy distribution. The formal similarity with B–E statistics becomes evident when Eq. (6) is integrated to yield the following rate expression:

$$\dot{n}(t) = -\frac{\lambda}{b}\frac{1}{A\exp(\lambda t) - 1}, \tag{7}$$

where $A = (1 - \lambda/b\dot{n}_0) = 1 + \varepsilon$, with $\varepsilon \ll 1$ representing an inverse measure of the extension of the process along the log t axis. For t values well below $1/\lambda = \tau$ and $A \approx 1$, one finds $\dot{n}t = \mathrm{d}n/\mathrm{d}\ln t = 1/b = F$. As shown in Ref. [5] the latter quantity is the maximum slope of the sigmoid $n(\ln t)$ plots. A straight line with this slope defined as $n_0 = F\ln(t_{\max}/t_{\min})$ provides a somewhat crude but useful description of the integral of Eq. (7) in the $n(\ln t)$ representation. The times $t_{\max} = 1/\lambda = \tau$ and $t_{\min} = 1/b|\dot{n}_0| = F/|\dot{n}_0|$.

The integral of the rate equation (7) to be used here as the relaxation function f_k ($k = 1,\ 3,\ 4$) reads with the already explained meaning of the symbols as follows:

$$f_k(t,0) = \frac{n_k(t)}{n_k^0} = 1 - \frac{\ln\left[1 + \varepsilon_k^{-1}(1 - \mathrm{e}^{-\lambda_k t})\right]}{\ln\left[1 + \varepsilon_k^{-1}\right]}. \tag{8}$$

According to this model the stretching of the macroscopic process is due to the clustering of the elementary transitions caused by the induction mechanism underlying Eqs. (6)–(8). Apart from single elementary transitions, involving only one relaxing unit, also double, triple, etc. transitions can take place, leading to correspondingly shortened τ values. For double transitions the relaxation time is $\tau/2$, for triple $\tau/3$, etc. The overall effect is an extension of the τ-spectrum towards times shorter than $\tau = 1/\lambda$ appearing in the basic equations above. In this respect the cooperative mechanism differs from the time course described by a KWW function, where the stretching effect extends to both sides of τ.

The notion that a cooperative mechanism of the above type can be applied to the time evolvement of a system of discrete relaxing units may need some comments. In the first place we note that the basic idea behind statistical distributions of B–E or Fermi–Dirac (F–D) is rather general and not limited to phenomena involving quantum mechanics. For instance, when analyzing sorption processes the exclusion principle of F–D statistics appears to be a useful tool taking into account the effect of the occupation of sorption sites [9]. In contrast to this there appears to be no attempts to exploit the equally plausible inclusion mechanism of B–E statistics in modeling time-dependent phenomena in solids, where independent processes are unlikely to occur, and where such a mechanism seems to offer a qualitative statistical picture of the cooperative motion of the relaxing units, about which there is a general agreement. Considering the limitations imposed on the motion of these units by the free volume, it is not unreasonable to assume that a successful activation of a unit leads not only to a single transition, but facilitates simultaneous transitions of other units in its vicinity. This is the basic idea behind Eq. (6) leading in a natural way to the formation of multiple elementary transitions. The size distribution of the transition clusters has been calculated in Refs. [5–8], where it has been shown that simple transitions are still the most numerous ones, and that the frequency of larger clusters decreases as 1/size. If n denotes the total number of units in a relaxing system, then the relaxation rate expressed in terms of the decreasing number of clusters, $\dot{m}$, is simply $\dot{m} = -\lambda n$, implying that n is partitioned among a smaller number of successful activations. From Refs. [5–8] further follows the expected result that the clustering tendency decreases with time. A stochastic treatment of the evolution of a macroscopic ensemble in terms of the master equation accounting for the B–E enhancement has been presented in Ref. [6].

The cooperative model employed here is well suited to describe the commonly observed linear variation of the relaxing quantity with logarithmic time. Stress relaxation in solids and the consolidation of volume in polymers following a cooling step may be mentioned as typical instances of such behavior. Stress relaxation in solids appears to exhibit a remarkable degree of similarity between different materials, including both polymers and metals, with regard to the extension of the process along the log t axis. As discussed in Refs. [5–8] and exemplified in Ref. [10], the inflexion slope, F, of relaxation curves plotted as stress vs. logarithmic time is proportional to the initial effective stress, n_0^*, in the following way:

$$F = (\mathrm{d}n/\mathrm{dln}\, t)_{\max} = (0.1 \pm 10\%)n_0^*. \quad (9)$$

The term effective stress denotes the difference between the initial applied stress, n_0, and the equilibrium stress, n_∞, reached after sufficiently long measuring times. For polymers, Eq. (9) is valid with the provision that the experimental data do not relate to temperatures close to T_g. In such cases the constant of proportionality in this equation tends to take on larger values, implying a narrowing of the corresponding distribution of relaxation times [10]. The normal value of this constant, as given by Eq. (9), defines a relaxation process extending over around 4.3 decade of time when approximated by a straight line tangent to the inflexion region.

Interesting is also the $\dot{n}(n)$ dependence following from the cooperative model. By integration of Eq. (6) using $\mathrm{d}\dot{n}/\mathrm{d}n = \ddot{n}/\dot{n}$ one finds:

$$\dot{n} = -\frac{\lambda}{b}[\exp(bn) - 1]. \quad (10)$$

This equation is nearly equivalent to the sinh-relations resulting from models where the activation energy is assumed to depend in a linear manner on the relaxing quantity, and where the final result is the logarithmic time law already mentioned.

Finally we note that the interpretation of the experimentally confirmed Eq. (9) in terms of the cooperative model leads to the remarkable result that the average relaxation time $\overline{\tau}$ taken over the entire process is 1/6 of the τ-values of single transitions or, which is the same, that the average size of the clustered transitions is 6 [8]. It may be added that Eq. (9), when translated into the formalism of the KWW function, corresponds to a stretching exponent $\beta \approx 0.27$ (= e/10).

4. Experimental

The polymer used was poly(methyl methacrylate) (*a*-PMMA, Plexiglas 6N, Rohm GmbH), density $\rho = 1190\ \mathrm{kgm^{-3}}$, $M_w = 90$ kg/mol, $M_w/M_n = 1.97$. The polymer contained 6 mol% of methyl acrylate distributed at random as determined by ^{13}C NMR [11].

The dilatometric measurements were carried out using mercury-in-glass dilatometry (MIG) constructed according to ASTM Standard D 864-52. The PMMA specimen was prepared by compression molding and ground to form a bar with a cross-section of approximately 6×6 mm (volume 3.24 cm^3). The specimen was inserted into the dilatometer which was then sealed and filled with filtrated high purity mercury (>99.999%) under vacuum of about 2 Pa. All temperature programs involving temperature scans and isothermal annealing were performed in a precision thermostatic bath (GRAND W14, Grand Instrument, Shepreth, UK), filled with silicon oil, where the dilatometer was immersed. The temperature fluctuations of the bath reported by the manufacturer were ±0.004 °C. The accuracy of the volume measurement was calculated to be about 1×10^{-5} cm^3/cm^3. The selected cooling rate was 0.3 °C/min, the heating rate 3 °C/min. Erasing of the thermal histories of PMMA was done by isothermal annealing at 120 °C for 15 min. Temperature up-scans were performed after isothermal relaxation at 75 °C for 0, 192 and 1204 h (aging time).

The measurements of the specific heat capacity were carried out using Perkin–Elmer DSC 1 Pyris analyzer. The temperature and heat flow were calibrated using indium standard, the values of specific heat capacity with the sapphire standard. The DSC samples, weight about 6 mg, were covered in aluminium foil and held in the thermostatic bath by a strainer. The temperature programs like erasing of the thermal histories, cooling and the relaxation were done in the thermostatic bath together with the dilatometer. The final temperature up-scans of the relaxed samples at 75 °C were performed in the DSC device at a rate of 3 °C/min.

The values of the bulk modulus were extracted from the volume–temperature isobars recorded at 20–120 MPa using a piston-die type *pvT* instrument (PVT 100 analyzer, SWO Polymertechnik GmbH, Krefeld, Germany). The temperature range was from 150 to 60 °C, the isobaric cooling rate 5 °C/min. Isobars relating to atmospheric pressure were extrapolated using Tait's equation of state included in the software of the instrument.

5. Results

The volumetric and calorimetric data shown in Figs. 1 and 2 display the commonly observed peaks in the volumetric coefficients of thermal expansion (CTE), $\alpha_p = ((1/v)(\partial v/\partial T))_p$ (derivatives are taken at constant pressure p), and the isobaric specific heat capacity, $c_p = (\partial h/\partial T)_p$, appearing in the vicinity of the glass transition temperature, T_g. In both cases the intensity of these peaks increases with the length of the aging period during which the specimens were kept at a temperature of 75 °C. The change in intensity is accompanied by a shift towards higher temperatures. From the experimental point of view an important difference between the two sets of graphs may be noted. While the $\alpha_p(T)$ data in Fig. 1 have been obtained by differentiating the $v(T)$ records produced by the dilatometer, the $c_p(T)$ results in Fig. 2 are direct recordings of the DSC device used.

The data in Figs. 1 and 2 are central to the modeling procedure, since they allow an easy and accurate determination of the peak position appearing as a reference temperature in the calculations. This would not be possible when using the corresponding $v(T)$ and $h(T)$ plots shown in Figs. 3 and 4.

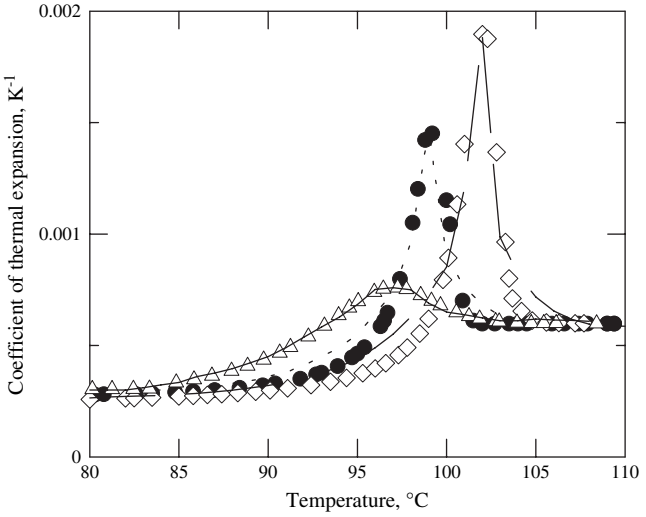

Fig. 1. Comparison of the measured volumetric coefficient of thermal expansion (symbols) with calculated predictions (lines) by means of Eqs. (1)–(5) and (8) for PMMA samples aged for different times. The symbol △ and the solid line – no aging, ● and the dotted line – 192 h aging, ◇ and the dashed line – 1204 h aging.

Again there is a basic difference between these two sets of plots, the $v(T)$ dependence representing a direct recording produced by the dilatometer, whereas the $h(T)$ data were calculated by integration of the underlying c_p values recorded by the DSC device.

For the sake of clarity we note that a single specimen was used in all the volumetric records shown in Figs. 1 and 3, whereas separate DSC specimens were employed for each temperature up-scan. There appears to be no reason to assume that this would affect the results. The same applies to the marked difference in size between the samples used in the two types of measurements.

Apart from experimental data, Figs. 1–4 also include the temperature dependence of the quantities in question

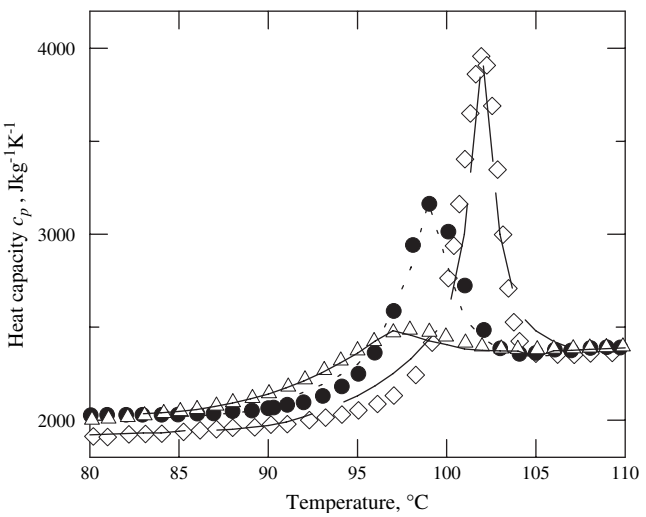

Fig. 2. Comparison of the measured specific heat capacity (symbols) with calculated predictions (lines) for samples aged for different times. Symbols and lines as in Fig. 1.

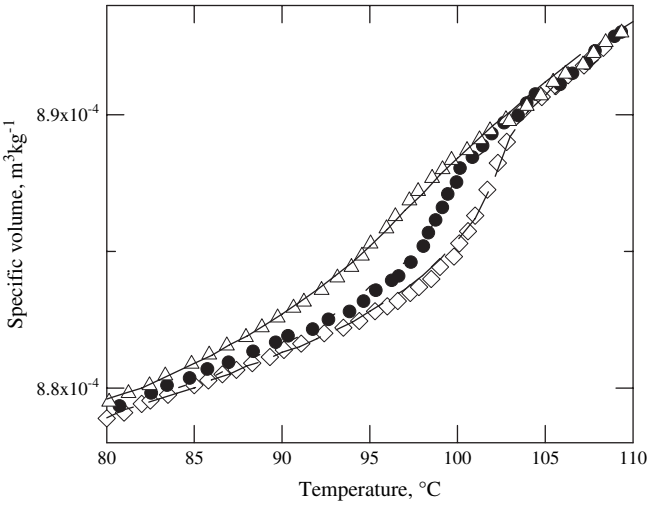

Fig. 3. Comparison of the measured volume evolution (symbols) with calculated predictions (lines) for samples aged for different times. Symbols and lines as in Fig. 1.

calculated using the thermodynamic scheme represented here by Eqs. (1)–(5) and introduced in detail in Refs. [3,4]. As can be seen a high degree of accuracy is attained in emulating the experimentally observed behavior recorded in temperature up-scans following 0, 192 and 1204 h of aging time at 75 °C.

The physical parameters of PMMA at the reference temperature needed for the predictive calculations are tabulated in Table 1 as the glassy and equilibrium (rubbery) reference temperature values. The parameters are identified for each set of experimental data corresponding to the aging time history, according to procedures explained in detail in Ref. [4] and illustrated in Fig. 5 for the coefficients of thermal expansion at the reference temperature and their temperature dependence. In some cases, the difference between the physical parameters related to the particular reference temperatures and thereby to the corresponding aging time is marginal.

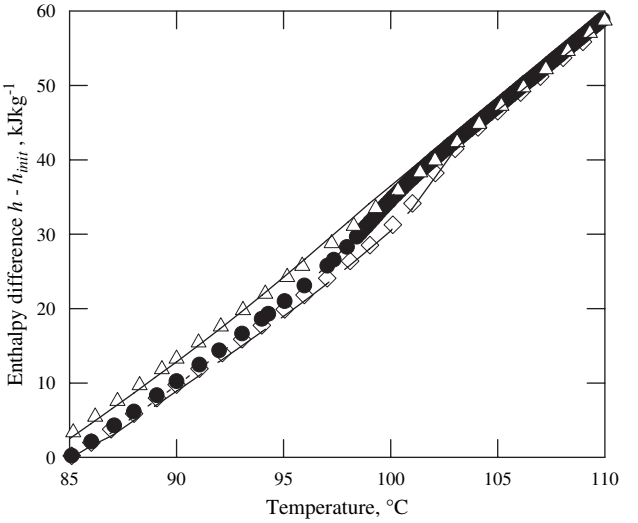

Fig. 4. Comparison of the measured enthalpy difference (symbols) with calculated predictions (lines) for samples aged for different times. Symbols and lines as in Fig. 1.

Table 1
The parameters and material characterization

Parameter	Units	All PMMA samples	Sample aging time, h		
			0	192	1204
T_{ref}	°C		97	99	102
ρ_{ref}	kg m^{-3}	1128			
α_{ref}	K^{-1}		7.57×10^{-4}	1.45×10^{-3}	1.89×10^{-3}
α_g^{ref}	K^{-1}		5.1×10^{-4}	4.2×10^{-4}	3.5×10^{-4}
α_∞^{ref}	K^{-1}	6.2×10^{-4}			
K_g^{ref}	GPa	2.45			
K_∞^{ref}	GPa	2.05			
c_{p_g}	J kg^{-1} K^{-1}	2080			
c_{p_∞}	J kg^{-1} K^{-1}	2380			
c_p^{ref}	J kg^{-1} K^{-1}		2480	3170	3960
$c_{p_g}^{ref}$	J kg^{-1} K^{-1}	2150			
$c_{p_\infty}^{ref}$	J kg^{-1} K^{-1}	2380			
$(\partial\alpha_\infty/\partial T)_p$	K^{-2}	0			
$(\partial\alpha_g/\partial T)_p$	K^{-2}		1.76×10^{-5}	6.32×10^{-6}	2.27×10^{-6}
$(\partial c_{p_\infty}/\partial T)_p$	J kg^{-1} K^{-2}	2.9			
$(\partial c_{p_g}/\partial T)_p$	J kg^{-1} K^{-2}	8			
$(\partial K_\infty/\partial T)_p$	MPa K^{-1}	−5.7			
$(\partial K_g/\partial T)_p$	MPa K^{-1}	−12			
C_1	Unitless	20			
U_C^{ref}	J kg^{-1}	9000			

When this difference is less than 2%, the parameter values for the aging times 0, 192 and 1204 h are for simplicity represented by one average value.

The coefficients C_1 and U_c^{ref} in Table 1, which are related to Williams, Landel, and Ferry (WLF) parameters [3,4], determine the material time scale, Eq. (11). The WLF parameters values given in Refs. [12–14] for PMMA lead to the justifiable choice, $C_1 = 20$ and $C_2 = 50$ K. Consequently, the rubbery shift factor, determined from the WLF equation, can be fitted by the relationship above Eq. (11) which gives $U_c^{ref} = 9000$ J kg^{-1}. This value of the equilibrated potential energy contribution to the internal energy at the reference temperature, U_c^{ref}, is considered constant in the computation despite its slight changes with the corresponding density at the respective reference temperature. The reason is that according to our calculations the predictions in Figs. 1–4 are not sensitive to the subtle variation of the WLF parameters and the potential energy $U_c^{ref} = U_{\infty\,pot}(\rho_{ref}, T_{ref})$. The same view is mentioned in Ref. [4].

The reference temperature T_{ref}, to which the parameters and their temperature dependence are extrapolated, is chosen to correspond to the CTE peak temperature of samples aging for different times. This choice is made to find the optimal representation of all data.

A comparison of our experimental data for PMMA with the published ones shows a good agreement. Our glassy CTE values depend on the aging time lying in the range $2.6–3.0 \times 10^{-4}$ K^{-1} with the equilibrium value $\alpha_\infty = 6.2 \times 10^{-4}$ K^{-1}. Rate-dependent glassy CTE values $\alpha_g = 2.46–2.35 \times 10^{-4}$ K^{-1} at cooling rates between 2 and 0.05 °C/min, and the equilibrium value $\alpha_\infty = 5.76 \times 10^{-4}$ K^{-1} are reported in Ref. [15]. For the same grade of PMMA as used in the present work $\alpha_g = 2.17 \times 10^{-4}$ K^{-1} and $\alpha_\infty = 6.14 \times 10^{-4}$ K^{-1} are given in Ref. [16], and $\alpha_g = 2.04 \times 10^{-4}$ K^{-1} and $\alpha_\infty = 6.07 \times 10^{-4}$ K^{-1} in Ref. [17]. Finally, CTE values in the range $2.25–2.72 \times 10^{-4}$ K^{-1} and $5.60–5.80 \times 10^{-4}$ K^{-1} below and above T_g, respectively, have been compiled in Ref. [18].

The measured values of equilibrium and glassy heat capacity and their difference are similar to data given in Refs. [17–23]. Our results yield the difference $c_{p_\infty} - c_{p_g} = 300$ J kg^{-1} K^{-1} which agrees well with published data lying in the range 300 J kg^{-1} K^{-1} ± 10%. The equilibrium heat capacity value, $c_{p_\infty} = 2380$ J kg^{-1} K^{-1}, is about 20% higher than 1950–2060 J kg^{-1} K^{-1} as given in Refs. [18,21,22]. This applies also to the glassy heat capacity $c_{p_g} = 2080$ J kg^{-1} K^{-1} differing from 1680–1780 J kg^{-1} K^{-1} as found in Refs. [18,21,22].

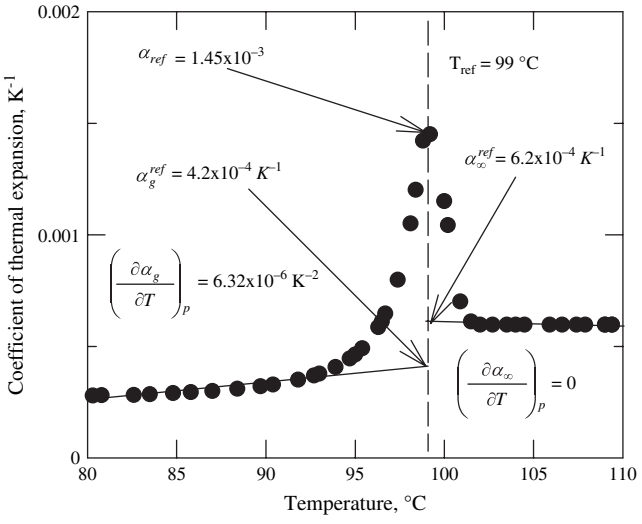

Fig. 5. The experimental values of temperature-dependent volumetric coefficient of thermal expansion through the glass transition for aging time 192 h and the illustration of its rubbery and glassy values at the reference temperature.

The values of the measured temperature dependence of the bulk modulus K have been compared with available data in Ref. [24]. The difference between our data given in Table 1 and published equilibrium values of K was less than 10%. Good agreement was found with regard to the temperature dependence of K in equilibrium. Our glassy values of K differ up to 25% from published data depending on the method used (isothermal, isobaric) [16,18,24,25]. The temperature dependence of K in the glassy state is again in good agreement with literature data [24].

Table 2 summarizes the values of the expansion terms of the equilibrium contribution to the stress (2) and the entropy (4). The majority of the expansion terms $(\psi_{II}, \psi_{IT}, \psi_{TT}, \psi_{IIT}, \psi_{ITT})$ is expressed in Ref. [4] as the functions of the equilibrium physical parameters listed in Table 1. Similarly, the terms ψ_{TTT} and ψ_{TTTT} relate to the temperature dependence of the equilibrium heat capacity $c_p(T)$ through the equilibrium physical parameters. Their values are adjusted in this paper to represent optimally the measured linear temperature dependence of the equilibrium $c_p(T)$ at temperatures over 105 °C. The values of $(\partial\psi_3/\partial T)^{\mathrm{ref}}_{I_H}$, $(\partial\psi_3/\partial I_H)^{\mathrm{ref}}_{T}$ presented in Table 2 are also determined by means of the algebraic relationships with the glassy physical parameters [4]. Similarly, the expansion terms $(\partial^2\psi_3/\partial T^2)^{\mathrm{ref}}_{I_H}$, $(\partial^2\psi_3/\partial I_H^2)^{\mathrm{ref}}_{T}$, $(\partial\psi_4/\partial T)^{\mathrm{ref}}_{I_H}$, $(\partial^2\psi_4/\partial T^2)^{\mathrm{ref}}_{I_H}$ are related to the temperature dependence of the glassy physical parameters. Nevertheless, their values are adjusted in this paper to represent optimally the measured temperature dependence of glassy $\alpha_p(T)$ and $c_p(T)$ below T_{ref}. This adjustment is similar to the modification of various parameters listed in Table 6 in Ref. [4]. Finally, there are only the relaxation function parameters ε_k and λ_k in Table 2, which are not related to the physical parameters listed in Table 1. The values of these parameters are determined by optimization of the correspondence between the experimental plots and predictions in Figs. 1–4. Although the number of the parameters and expansion terms in Tables 1 and 2 may seem high, their determination from the separately measured material properties is straightforward. The specific step that contributes to a proper description of the experimental data in Figs. 1–4 is the choice of the reference temperature, which is taken equal to the temperature of the peaks in thermal expansion and specific heat.

Table 2
The values of expansion terms and relaxation function parameters

Constant	Units	All PMM samples	Sample aging time, h		
			0	192	1204
ψ_{II}	J kg^{-1}	1.82×10^{6}			
ψ_{IT}	J kg^{-1} K^{-1}	-1.12×10^{3}			
ψ_{TT}	J kg^{-1} K^{-2}		5.6	5.3	5.3
ψ_{IIT}	J kg^{-1}	-5.05×10^{3}			
ψ_{ITT}	J kg^{-1} K^{-2}	12.6			
ψ_{TTT}	J kg^{-1} K^{-3}		10^{-2}	1.5×10^{-2}	1.5×10^{-2}
ψ_{TTTT}	J kg^{-1} K^{-4}		-5×10^{-4}	0	0
ψ_1^{ref}	J kg^{-1}	3.55×10^{5}			
ψ_3^{ref}	J kg^{-1} K^{-1}		40.8	214	366
ψ_4^{ref}	J kg^{-1} K^{-2}		0.37	0.3	0.19
$(\partial\psi_3/\partial T)^{\mathrm{ref}}_{I_H}$	J kg^{-1} K^{-2}		−19.1	−7.87	−3.82
$(\partial\psi_3/\partial I_H)^{\mathrm{ref}}_{T}$	J kg^{-1} K^{-2}	-5.6×10^{3}			
$(\partial^2\psi_3/\partial T^2)^{\mathrm{ref}}_{I_H}$	J kg^{-1} K^{-3}		54	52	50
$(\partial^2\psi_3/\partial I_H^2)^{\mathrm{ref}}_{T}$	J kg^{-1} K^{-3}	2.04×10^{5}			
$(\partial\psi_4/\partial T)^{\mathrm{ref}}_{I_H}$	J kg^{-1} K^{-3}	2.2×10^{-2}			
$(\partial^2\psi_4/\partial T^2)^{\mathrm{ref}}_{I_H}$	J kg^{-1} K^{-4}	1.77×10^{-5}			
ε_1	Unitless	10^{-3}		10^{-3}	10^{-3}
λ_1	s^{-1}	10^{-3}		10^{-5}	10^{-5}
ε_3	Unitless	10^{-3}		10^{-3}	10^{-3}
λ_3	s^{-1}	10^{-2}		10^{-4}	10^{-4}
ε_4	Unitless	10^{-3}		10^{-3}	10^{-3}
λ_4	s^{-1}	10^{-3}		10^{-5}	10^{-5}

The predictions in Figs. 1–4 were computed by an iterative procedure using *Mathematica* Version 4. The iteration of the system of Eqs. (1) and (3) follows the same procedure as used in Ref. [4] with the exception that the relaxation functions are not represented by the stretched exponential functions as in Ref. [4] but by the expression (8), that is, the functions emerging from the cooperative model discussed in Section 3.

The double integral terms associated with the Helmholtz free energy ψ contribution to the potential (configurational) energy, $U_c = U_{\infty_{\mathrm{pot}}} + (\psi - \psi_\infty) + T(\eta - \eta_\infty)$, are negligible for isobaric tests [3]. Thus in our case the potential energy U_c that governs the shift factor, $\log a = C_1((U_c^{\mathrm{ref}}/U_c) - 1)$, and consequently, the material time,

$$t^* - s^* = \int_s^t \frac{\mathrm{d}x}{a(x)}, \tag{11}$$

is considered to equal $U_c = U_{\infty_{\mathrm{pot}}} + T(\eta - \eta_\infty)$. For evaluating $U_{\infty_{\mathrm{pot}}}$ the "glassy" limit assigning the glassy values to the cross-term prefactors, Eq. (66) in [3], is used in the computation.

As mentioned above, the parameters ε_k and λ_k in the normalized relaxation function f_k ($k = 1, 3, 4$) have to be found by optimization in order to provide best representation of experimental data in Figs. 1–4. As explained in Section 3 describing the cooperative model, the quantities ε_1, ε_3 and ε_4 represent an inverse measure of the extension of the underlying process along the log t axis. As evident from Table 2, the experimental results were properly described when using $\varepsilon_k = 10^{-3}$ for all the three relaxation functions. The calculation did not reveal any significant change in these ε_k values with aging time, implying a constant width of about three decades of the corresponding τ_k spectrum.

The second parameter of the relaxation model, λ_k, is the inverse of the relaxation time τ_k. In our case this is the τ_k-value relating to simple elementary events, thus limiting the τ_k spectrum at its higher end, and fixing its position along the time axis. In contrast to ε_k, a distinct dependence of λ_k on aging is noted. As shown in Table 2, the rates λ_1, λ_3 and λ_4 relating to the bulk modulus, thermal expansion and heat capacity relaxation functions, respectively, are lowered by the aging process by a factor 10^{-2}.

On a qualitative level we thus arrive at the expected result that without the consolidation of the sample at the aging temperature, and thus no entropy relaxation and no decrease in the potential energy $U_c = U_{\infty_{\mathrm{pot}}} + T(\eta - \eta_\infty)$, the transition to the

equilibrium state is facilitated. The role of the entropic relaxation is reflected by the relaxation function f_3 which governs the isothermal relaxation as follows from Eq. (3) when the temperature-dependent term is eliminated. The rate entering this function is an order of magnitude larger than the rates λ_1 and λ_4.

From the ε_k and λ_k values in Table 2 one may conclude that the relaxation time spectrum underlying the measured data retains its width while shifting to longer times as the aging period is extended. This is, in essence, what is normally found when determining the effect of aging on viscoelastic phenomena, such as creep, stress relaxation or dynamic mechanical properties [26,27].

6. Conclusions

The application of the rational mechanics scheme presented by Caruthers et al. [3] and Adolf et al. [4] to the volumetric and enthalpic behaviors of *a*-PMMA during temperature upscans following different periods of aging (0, 192, and 1204 h) produced good agreement between experimental results and theoretical predictions. This applies both to the dilatometric (mercury-in-glass) and DSC data presented as $v(T)$ and $h(T)$ graphs and their differential counterparts, that is, $\alpha(T)$ and $c_p(T)$. The intensity and position of the peaks appearing in the latter graphs was properly emulated by the theory.

The original theoretical framework [3,4] was slightly modified by replacing the stretched exponential representation of the time dependence of the thermodynamic quantities by a simple cooperative model based on a model reminiscent of B–E statistics. The effect of aging was reflected in a shift of the corresponding distribution of relaxation times, τ, towards longer τ values, while the width of the τ distribution remained constant. The relaxation parameters appear to assume reasonable values, considering the fact that they were obtained by evaluation of volumetric and enthalpic data recorded during a temperature up-scan.

Acknowledgements

This work was financially supported by the Grant Agency of the Czech Republic (Grant No. 103/05/0803), project MSM7088352101, and the Institute of Hydrodynamics Fund AV0Z20600510.

References

[1] Simon SL, Bernazzani P. J Non-Cryst Solids 2006;352:4763–8.
[2] Andreozzi L, Faetti M, Giordano M, Palazzuoli D, Zulli F. Macromolecules 2003;36:7379–87.
[3] Caruthers JM, Adolf DB, Chambers RS, Shrikhande P. Polymer 2004;45:4577–97.
[4] Adolf DB, Chambers RS, Caruthers JM. Polymer 2004;45:4599–621.
[5] Kubát DG, Bertilsson H, Kubát J, Uggla S. Rheol Acta 1992;31:390–8.
[6] Kubát MJ, Riha P, Rychwalski RW, Kubát J. Europhys Lett 2000;50:507–12.
[7] Kubát MJ, Riha P, Rychwalski RW, Uggla S. Mech Time-Depend Mater 1999;3:31–47.
[8] Rigdahl M, Riha P, Rychwalski RW, Kubát MJ, Kubát J. Mech Time-Depend Mater 2004;8:95–103.
[9] Kirchheim R. Macromolecules 1992;25:6952–60.
[10] Kubát J, Rigdahl M. Stress relaxation behavior of solid polymers. In: Brostow W, Corneliussen RD, editors. Failure of plastics. New York: Hanser Publishers; 1986. p. 60–83.
[11] Schantz S. Macromolecules 1997;30:1419–25.
[12] Fuchs K, Friedrich C, Weese J. Macromolecules 1996;29:5893–901.
[13] Kopesky ET, Haddad TS, Cohen RE, McKinley GH. Macromolecules 2004;37:8992–9004.
[14] Miwa Y, Yamamoto K, Sakaguchi M, Sakai M, Makita S, Shimada S. Macromolecules 2005;38:832–8.
[15] Greiner R, Schwarzl FR. Rheol Acta 1984;23:378–95.
[16] Schmidt M, Maurer FHJ. J Polym Sci Part B Polym Phys 1998;36:1061–80.
[17] Vernel J, Rychwalski RW, Pelíšek V, Sáha P, Schmidt M, Maurer FHJ. Thermochim Acta 1999;342:115–37.
[18] Brandrup J, Immergut EH. Polymer handbook. 3rd ed. New York: John Wiley and Sons; 1989.
[19] Song M, Hammiche A, Pollock HM, Hourston DJ, Reading M. Polymer 1995;36:3313–6.
[20] Agari Y, Ueda A, Omura Y, Nagai S. Polymer 1997;38:801–7.
[21] Theobald S, Pechhold W, Stoll B. Polymer 2001;42:289–95.
[22] Hempel E, Beiner M, Huth H, Donth E. Thermochim Acta 2002;391:219–25.
[23] Chuai C, Almdal K, Lyngaae-Jorgensen J. J Appl Polym Sci 2004;91:609–20.
[24] Slobodian P, Riha P, Rychwalski RW, Emri I, Sáha P, Kubát J. Eur Polym J 2006;42:2824–37.
[25] Zoller P, Walsh D. Standard pressure–volume–temperature data for polymers. Technomic Publ Co; 1995.
[26] Struik LCE. Physical aging of amorphous polymers and other materials. Amsterdam: Elsevier; 1978.
[27] Hutchinson JM. Prog Polym Sci 1995;20:703–60.